CRYSTAL GROWTH & DESIGN

Article

pubs.acs.org/crystal

Highly Enhanced Gas Uptake and Selectivity via Incorporating Methoxy Groups into a Microporous Metal−Organic Framework

Published as part of a Crystal Growth and Design virtual special issue on Crystal Engineering of Nanoporous Materials for Gas Storage and Separation

Hui-Min Wen,[#,†] Ganggang Chang,[#,†] Bin Li,[*,†] Rui-Biao Lin,[†] Tong-Liang Hu,[‡] Wei Zhou,[§] and Banglin Chen[*,†]

[†]Department of Chemistry, University of Texas at San Antonio, One UTSA Circle, San Antonio, Texas 78249-0698, United States

[‡]School of Materials Science and Engineering, National Institute for Advanced Materials, Collaborative Innovation Center of Chemical Science and Engineering (Tianjin), Nankai University, Tianjin 300071, China

[§]NIST Center for Neutron Research, National Institute of Standards and Technology, Gaithersburg, Maryland 20899-6102, United States

Supporting Information

ABSTRACT: A porous metal−organic framework $[Cu_2L(H_2O)_2]\cdot 7DMF\cdot 4H_2O$ (**UTSA-90**, H_4L = 2′,5′-dimethoxy-[1,1′:4′,1″-terphenyl]-3,3″,5,5″-tetracarboxylic acid) functionalized with methoxy groups has been successfully constructed and structurally characterized, which is isoreticular to **NOTT-101**. A single crystal structure determination reveals that the incorporation of bulky methoxy groups can efficiently split the large pores and channels of **NOTT-101a** into smaller ones within **UTSA-90**. Compared with **NOTT-101a**, the activated **UTSA-90a** exhibits the significantly enhanced C_2H_2 (214 vs 184 $cm^3\ g^{-1}$) and CO_2 (125 vs 83 $cm^3\ g^{-1}$) adsorption capacities at 295 K and 1 bar. It is worth noting that the CO_2 uptake of **UTSA-90a** represents the highest reported for all the NbO-type metal-organic frameworks (MOFs). In addition, **UTSA-90a** also shows a significant enhancement in adsorptive selectivities for the separation of C_2H_2/CH_4, CO_2/CH_4, and CO_2/N_2 mixtures at ambient conditions. This work indicates that introducing bulky functional groups on the linker might be a promising approach to tune pore sizes and environments in MOFs for enhancing their gas adsorption and separation properties.

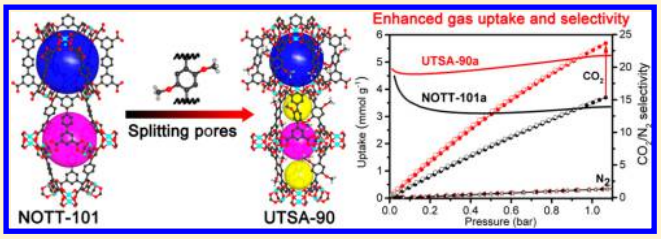

INTRODUCTION

The emergence of crystalline porous metal−organic frameworks (MOFs) has attracted much attention in the last two decades for their particularly useful applications on gas storage and separation.[1−5] The relatively simple and architectural chemistry enables us to achieve intricate design and precise control over porosity, pore size/shape, and functionality of MOF materials.[6−15] It is very important in the chemistry and materials science communities to realize new materials or strategies to effectively improve gas sorption and separation capacities and thus to optimize their specific properties for diverse purposes. Generally, the effects of functional groups with high polarity, such as Lewis basic N sites, amide, −OH, $-NH_2$, etc., and/or open metal sites decorating the pores of MOFs have been well documented to enhance gas uptake and separation capacities, since some gas substrates, like CO_2, C_2H_2, etc., possess a large quadrupole moment and these functional sites are able to induce polarization and thus enhance the binding affinity.[16−31] Another important way to improve gas sorption and selectivity is precise control and fine-tuning of pore/channel sizes within porous MOFs at the molecular level.[32,33] In this regard, control of framework interpenetration and judicious selection of organic linkers are two general strategies.[34−37] For example, Zaworotko et al. utilized the above two strategies to finely tune pore sizes in SIFSIX series and found that **SIFSIX-3-Zn** with narrow pore windows of 3.84 Å in diameter exhibit extremely high CO_2/CH_4 and CO_2/N_2 selectivities.[35] Chen and co-workers revealed that **UTSA-16** with small pore sizes of 3.3 × 5.4 $Å^2$ displays a significantly high volumetric uptake (160 $cm^3\ cm^{-3}$) of CO_2 under ambient conditions.[38] Apparently, the realization of porous materials with relatively small pore/window sizes is very important to target high gas sorption and separation capacities.[39−41]

Recently, several new strategies have been reported and developed to effectively partition large pores into small pores within MOF materials, which certainly led to significantly enhanced gas storage and separation properties.[42−47] For example, Feng and co-workers reported a new pore space

Received: January 23, 2017
Revised: February 20, 2017
Published: March 3, 2017

ACS Publications © 2017 American Chemical Society

DOI: 10.1021/acs.cgd.7b00111
Cryst. Growth Des. 2017, 17, 2172−2177

partition strategy to split large pores into smaller ones through the insertion of a secondary ligand into **MIL-88**, resulting in dramatically enhanced CO_2 uptakes to near-record values.[42,43] Wang and co-workers also partitioned the channels of **MOF-5** into confined and hydrophobic compartments by *in situ* polymerization of aromatic acetylenes for remarkably increased CO_2 adsorption and CO_2/N_2 selectivity at 273 K and 1 bar.[44] In addition, the immobilization of some bulky functional groups (e.g., methyl, *tert*-butyl) onto the frameworks have been demonstrated to be capable of finely tailoring the pore sizes and environments for gas storage and separation.[48−53] The representative example was that Chen and colleagues achieved a high C_2H_2/C_2H_4 separation in the family of mixed MOFs (**M′MOFs**) by grafting bulky *tert*-butyl groups into the linkers for finely tuning the pore spaces.[48] Inspired by their works, herein we designed and incorporated the bulky methoxy groups (−OMe) into the framework of **NOTT-101** to form a porous MOF material (termed as **UTSA-90**). Very interestingly, the incorporation of methoxy groups was able to partition the large pores and channels into smaller ones within **UTSA-90** for fine-tuning of pore spaces, which plays the most important role in trapping CO_2 and C_2H_2 molecules. As a result, the activated **UTSA-90a** exhibits not only notably improved C_2H_2 (214 $cm^3\ g^{-1}$) and CO_2 (125 $cm^3\ g^{-1}$) uptakes but also much better selectivities for separation of C_2H_2/CH_4 (60.1), CO_2/N_2 (21.7), and CO_2/CH_4 (5.3) mixtures at ambient conditions compared to those of **NOTT-101a**.

RESULTS AND DISCUSSION

The organic linker H_4L was readily synthesized through a Suzuki cross-coupling reaction of 1,4-dibromo-2,5-dimethoxybenzene and 2 equiv of 5-(4,4,5,5-tetra-methyl-1,3,2-dioxaborolan-2-yl) isophthalate similarly to the reported literatures,[54,55] followed by hydrolysis and acidification (Scheme 1).

Scheme 1. Synthetic Route to the Organic Linker H_4L

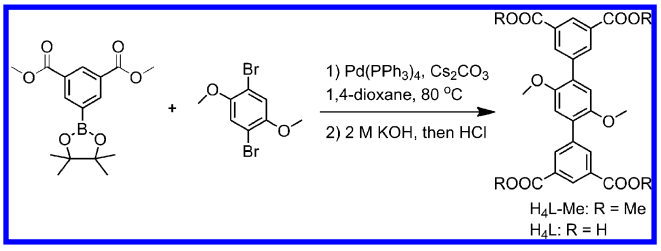

Solvothermal reaction of H_4L with $Cu(NO_3)_2{\cdot}2.5H_2O$ in DMF/MeCN/H_2O (6/1/1, v/v) under acidic conditions at 80 °C for 1 day afforded blue block crystals of **UTSA-90** in about 61% yield (based on the ligand). **UTSA-90** has a formula of $[Cu_2L(H_2O)_2]{\cdot}7DMF{\cdot}4H_2O$, as determined by single-crystal X-ray diffraction (XRD) analysis, thermogravimetric (TGA), and elemental analysis. UTSA-90 of different porosities and properties have been independently reported by other groups.[54,55] **UTSA-90** shows thermal stability up to 270 °C by TGA and the increased moisture stability.[54] The phase purity of the bulk sample was confirmed by powder X-ray diffraction (PXRD), where the measured PXRD patterns were in good agreement with the simulated ones from single-crystal diffraction data (Figure S3).

XRD analysis of single crystals of **UTSA-90** revealed that this framework crystallizes in the hexagonal space group $R\bar{3}m$, where the framework nodes consist of dinuclear $Cu_2(COO)_4$ secondary building units (SBUs) coordinated by the carboxylates of L^{4-} in paddlewheel fashion (Figure 1). **UTSA-90** forms a three-dimensional (3D) NbO-type topology, which is isoreticular to **NOTT-101**.[55] As shown in Figure 1a, the **NOTT-101** framework has two types of cages: one cage (blue) of about 11.2 $Å^2$ in diameter and the other large irregular elongated cage (pink) of about 9.6 × 22.3 $Å^2$. The incorporation of bulky methoxy groups into the linker of **NOTT-101** can remarkably alter the MOF pore structures. First, the diameter of the blue cage is significantly decreased from 11.2 Å in **NOTT-101** to 8.9 Å in **UTSA-90** because of six −OMe groups pointing into the cage (Figure 1b). Second, the large irregular cage can be divided into three small cages by two series of three −OMe groups in close contact: one squashed cuboctahedral cage at the center (pink) and two extraordinarily small cages of ∼3.5 Å on the top and bottom (yellow). Furthermore, the large pore channels in **NOTT-101** along the *a*- and *b*-axes can be also fragmented into numerous smaller channels by the grafted −OMe groups within **UTSA-90** (Figure 1c,d). These observed changes in pore spaces can be further confirmed by the calculated geometric pore size distributions (PSD) of **NOTT-101** and **UTSA-90** (Figure 2).[56] As depicted in Figure 2, when the −OMe groups are incorporated into the framework, the pores with widths of about 12 Å in **NOTT-101** diminish, whereas new pores with widths of 8.7 Å (reduced/partitioned pores) emerge in **UTSA-90**. These results suggest that the immobilized methoxy groups play important roles in the diminution and partition of pore spaces, which would certainly have a significant effect on gas adsorption and separation properties.

The permanent porosity of activated **UTSA-90a** was determined by nitrogen adsorption isotherms at 77 K. Before adsorption measurements, the as-synthesized sample was solvent-exchanged by dry acetone at least 10 times, and then heat treated at room temperature for 24 h and at 373 K for an additional 24 h under high vacuum to yield the desolvated **UTSA-90a**. As shown in Figure 3a, **UTSA-90a** exhibits a reversible type I character with a saturated N_2 adsorption capacity of about 562 cm^3/g at 77 K and 1 bar, corresponding to a pore volume of 0.88 $cm^3\ g^{-1}$. This value is very close to the calculated pore volume of 0.82 $cm^3\ g^{-1}$ from a single-crystal structure, indicating that the sample was desolvated completely. The Brunauer−Emmett−Teller (BET) surface area of **UTSA-90a** was found to be 2273 $m^2\ g^{-1}$. As expected, these values are much lower than those reported in the isoreticular **NOTT-101a** (1.08 $cm^3\ g^{-1}$ and 2805 $m^2\ g^{-1}$) because of the free volume occupation by the immobilized methoxy groups.

The established high porosity and fine-tuning over pore metrics in **UTSA-90a** have prompted us to examine its gas sorption properties. The single-component gas adsorption isotherms for **UTSA-90a** were collected up to 1 bar at 273 and 295 K, respectively (Figures 3b and S6). As shown in Figure 3b, **UTSA-90a** can adsorb an exceptionally high amount (214 $cm^3\ g^{-1}$) of C_2H_2 at 295 K and 1 bar, being notably higher than that of **NOTT-101** (184 $cm^3\ g^{-1}$). Table S1 further lists the comparison of **UTSA-90a** with some promising MOFs for C_2H_2 storage at ambient conditions. It can be seen from the table that the C_2H_2 uptake of **UTSA-90a** is among the highest reported for MOF materials to date and even outperforms those of two benchmark MOFs: **HKUST-1** (201 $cm^3\ g^{-1}$)[57] and **CoMOF-74** (197 $cm^3\ g^{-1}$).[58] Similarly, **UTSA-90a** also shows a significantly enhanced CO_2 uptake capacity (125 $cm^3\ g^{-1}$, 24.6 wt %) than **NOTT-101a** (83 $cm^3\ g^{-1}$, 16.5 wt %) at

DOI: 10.1021/acs.cgd.7b00111
Cryst. Growth Des. 2017, 17, 2172−2177

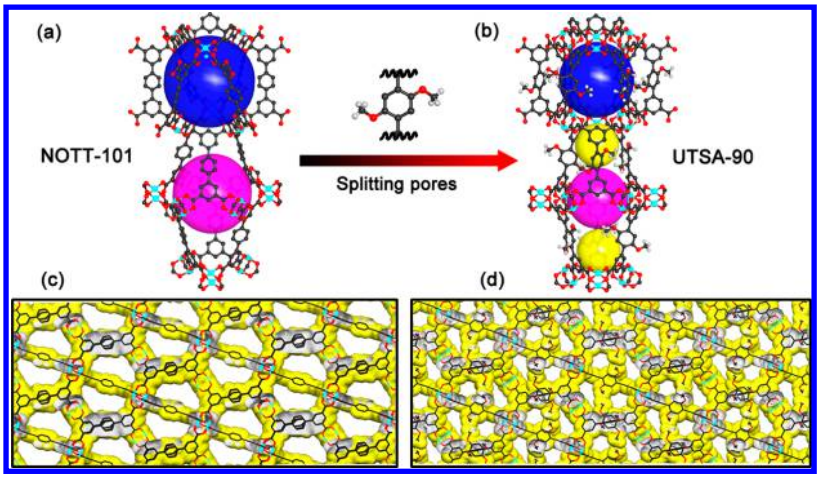

Figure 1. Comparison of crystal structures of **NOTT-101** and **UTSA-90**. (a, b) Detail of pore spaces in **NOTT-101** and **UTSA-90**, respectively, and (c, d) the channels of **NOTT-101** (c) and **UTSA-90** (d), viewed along the *a* and *b* axes, illustrating the changes of pore and channel sizes after introducing the bulky methoxy groups into the framework. Spheres denote the pores within the frameworks (turquoise: Cu, red: O, black, C and white, H).

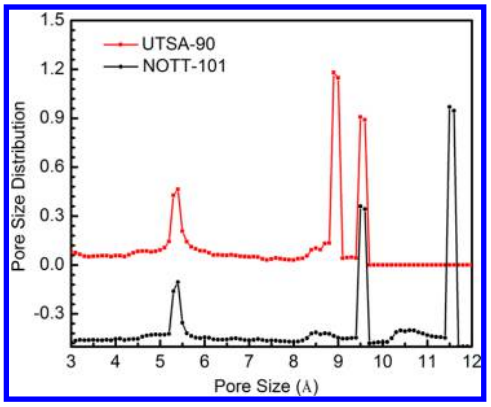

Figure 2. Pore size distributions of **UTSA-90** (red line) and **NOTT-101**(black line), calculated using the well-known method by Gubbins et al.[56] The van der Waals diameters of the framework atoms were adopted from the Cambridge Crystallographic Centre.

295 K and 1 bar. It should be pointed out that this gravimetric CO_2 uptake of **UTSA-90a** represents the highest value observed to date in the entire family of NbO-type MOFs (Table 1),[59−67] including those functionalized with strong affinity sites, for example, Lewis basic N sites,[60] amide,[64] amino,[63] methylol,[53] and so on. Compared with other types of MOFs, to the best of our knowledge, only a handful of MOFs such as **Mg-MOF-74** (178 $cm^3\ g^{-1}$),[68] **Co-MOF-74** (155 $cm^3\ g^{-1}$),[68] **MAF-X25ox** (159 $cm^3\ g^{-1}$),[69] **CPM-231** (151 $cm^3\ g^{-1}$),[70] **Cu-TDPAT** (132 $cm^3\ g^{-1}$),[71] and **Cu(Me-4py-trz-ia)** (136 $cm^3\ g^{-1}$)[72] have much higher CO_2 gravimetric uptake at ambient conditions (Table S2). In terms of volumetric uptake, the value of **UTSA-90a** is moderately high, reaching 96 $cm^3\ cm^{-3}$, but still superior to other reported NbO-type MOFs excluding **NbO-Pd-1** (Table 1).

The high C_2H_2 and CO_2 uptakes for **UTSA-90a** suggest that incorporating bulky methoxy groups plays an important role in enhancing gas sorption capacities. To better understand these observations, we calculated the coverage-dependent adsorption enthalpies of **UTSA-90a** for C_2H_2 and CO_2 below 1 bar by the well-established virial method. As shown in Figure S8, the initial Q_{st} values of C_2H_2 and CO_2 for **UTSA-90a** were estimated to be 36.5 and 20.5 kJ/mmol, respectively. The Q_{st} of C_2H_2 at

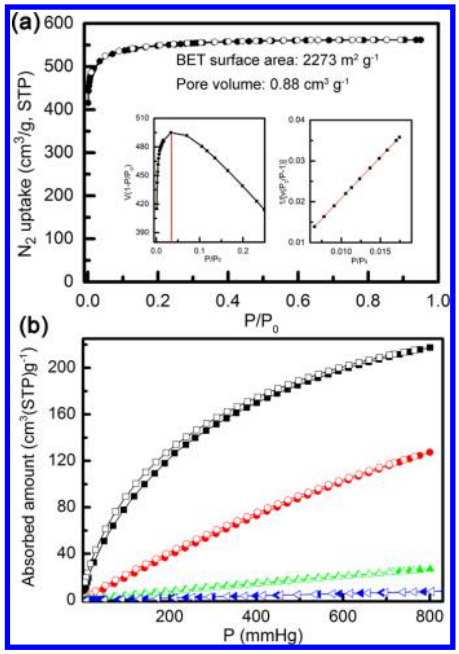

Figure 3. Gas sorption study on the activated **UTSA-90a**. (a) Nitrogen isotherm at 77 K with consistency and BET plots. (b) C_2H_2 (black), CO_2 (red), CH_4 (green), and N_2 (blue) sorption isotherms for **UTSA-90a** at 295 K.

zero coverage is close to that of **NOTT-101a** (37.1 kJ/mmol),[37] whereas the value of CO_2 is slightly lower than **NOTT-101a** (23.3) and those NbO-type MOFs with functional sites, such as **NbO-Pd-1** (24.8), **HKUST-1** (31.2), and **NOTT-125** (25.4). These results indicate that the immobilized methoxy groups may not offer additional strong adsorption sites to enforce the interaction with gas molecules. Therefore, the suitable pore sizes formed by the partition effect of methoxy groups within **UTSA-90a** are presumably responsible for the dramatically enhanced C_2H_2 and CO_2 uptake capacities. Such phenomena was also clearly exemplified by **UTSA-16** and **PCN-88** with moderate Q_{st} values for high CO_2 uptakes due to the optimized pore sizes for efficiently trapping CO_2 molecules.[38,73]

DOI: 10.1021/acs.cgd.7b00111
Cryst. Growth Des. 2017, 17, 2172−2177

Table 1. Comparison of CO_2 Uptake of UTSA-90a with Some Promising Cu-Based NbO-Type MOFs

MOFs	S_{BET} [m^2 g^{-1}]	V_p (g cm^{-3})	CO_2 uptake[a]		Q_{st}[b]	ref
			cm^3 g^{-1}	cm^3 cm^{-3}		
UTSA-90a	2273	0.88	125	96	20.5	this work
NbO-Pd-1	1568	0.60	124	116	24.8	59
ZJNU-44	2314	0.916	116	87		60
ZJNU-40	2209	0.88	108	80	18.4	61
QI-Cu	1631	0.662	102	85	23.7	53
NJU-Bai14	2384	0.924	100	75	24.5	62
ZJU-8a	2501	1.02	95	66	21.9	63
HNUST-1	1400	0.571	93	54	31.2	64
NOTT-125	2471	1.10	93	63	25.4	65
NOTT-101a	2805	1.08	83	58	23.3	61
SNU-50	2300	1.08	80	52	25.8	66
NU-135	2600	1.02	80	60	25.5	67

[a]At room temperature and 1 bar. [b]The CO_2 adsorption enthalpies at zero coverage.

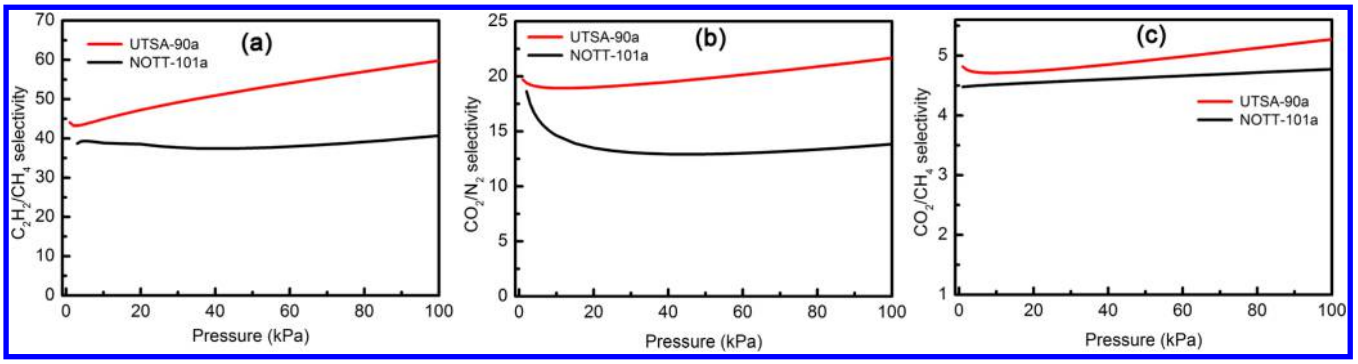

Figure 4. Comparison of IAST selectivities of (a) C_2H_2–CH_4 (50/50, v/v), (b) CO_2–N_2 (15/85, v/v), and (c) CO_2–CH_4 (50/50, v/v) mixtures between **UTSA-90a** and **NOTT-101a** at room temperature.

In sharp contrast to the high C_2H_2 and CO_2 uptake capacities, as depicted in Figure 3b, **UTSA-90a** shows little CH_4 (26 cm^3 g^{-1}) and N_2 (6.9 cm^3 g^{-1}) uptake at 1 bar and 295 K. The marked difference between CO_2/C_2H_2 and CH_4/N_2 adsorption isotherms indicates that **UTSA-90a** has a great potential for the separation of C_2H_2/CH_4, CO_2/CH_4, and CO_2/N_2 mixtures. The well-known Ideal adsorbed solution theory (IAST) was used to calculate the adsorption selectivity of **UTSA-90a** for the following three binary mixtures: C_2H_2–CH_4 (50/50, v/v), CO_2–CH_4 (50/50, v/v), and CO_2–N_2 (15/85, v/v), which are mostly related to acetylene purification, natural gas upgrading, and postcombustion CO_2 capture applications, respectively. Figure 4a–c presents the IAST selectivities of C_2H_2–CH_4, CO_2–N_2, and CO_2–CH_4 separation for **UTSA-90a** and **NOTT-101a** at room temperature. The adsorption selectivity of **UTSA-90a** for C_2H_2/CH_4, CO_2/N_2, and CO_2/CH_4 separation was found to be 60.1, 21.7, and 5.3, respectively (at 295 K and 1 bar), all of which show a significant improvement compared with those of **NOTT-101a** (40.8, 13.8, and 4.7). We note that the C_2H_2/CH_4 selectivity of 60.1 is much higher than most of other promising MOFs reported to date,[74] such as **FJI-C4** (51),[75] **UTSA-35a** (19),[76] and **ZJU-199** (27).[77] In addition, the IAST selectivity of CO_2/N_2 (19–22) for **UTSA-90a** is also very respectable, which outperforms any other reported NbO-type MOF (except **NbO-Pd-1**), even including those functionalized with Lewis basic N sites (**ZJUN-44**: 16.3),[60] oxamide (**NOTT-125a**: 16),[65] benzothiadiazole (**ZJNU-40**: 17),[61] and amino (**ZJU-8a**, 12.3).[63] Most importantly, this value is also comparable to that of some famous MOFs, for example, **Cu-BTTri** (21),[78] **Cu-TPBTM** (22),[19] **PCN-88** (18),[73] and **HKUST-1** (20),[79] suggesting its great potential for capturing CO_2 from flue gas. All the observed results indicate that the incorporation of bulky methoxy groups for splitting pore spaces within MOFs shows a great benefit not only for improving gas uptakes, but also for the selectivity of CO_2 and C_2H_2 over CH_4 and N_2 in the low pressure region.

CONCLUSIONS

In summary, we have designed and synthesized an organic linker with functional methoxy groups and successfully constructed its copper(II) metal–organic framework (**UTSA-90**). By introducing the bulky –OMe groups into the framework, fine tailoring of pore spaces can be achieved within **UTSA-90**, where the large pores and channels can be split into smaller ones. These partitioned pores played the most important role in enhancing gas adsorption and separation capacities. As a result, **UTSA-90a** exhibited not only significantly improved C_2H_2 and CO_2 uptakes but also much better selectivities for separation of C_2H_2/CH_4, CO_2/CH_4, and CO_2/N_2 mixtures than the isoreticular **NOTT-101a** at ambient conditions. Our work here demonstrates a promising strategy that the incorporation of bulky functional groups into MOF materials has the potential to finely tune the MOF pore sizes and metrics, and thus optimize their gas sorption and separation properties.

DOI: 10.1021/acs.cgd.7b00111
Cryst. Growth Des. 2017, 17, 2172–2177

■ ASSOCIATED CONTENT

Supporting Information

. The Supporting Information is available free of charge on the ACS Publications website at DOI: 10.1021/acs.cgd.7b00111.

Crystallographic data, NMR, TGA, PXRD, heats of adsorption, adsorption isotherms, and additional figures and tables (PDF)

Accession Codes

CCDC 1529733 contains the supplementary crystallographic data for this paper. These data can be obtained free of charge via www.ccdc.cam.ac.uk/data_request/cif, or by emailing data_request@ccdc.cam.ac.uk, or by contacting The Cambridge Crystallographic Data Centre, 12 Union Road, Cambridge CB2 1EZ, UK; fax: +44 1223 336033.

■ AUTHOR INFORMATION

Corresponding Authors

*(B.L.) E-mail: bin.li@utsa.edu.
*(B.C.) E-mail: banglin.chen@utsa.edu.

ORCID

Rui-Biao Lin: 0000-0003-3267-220X
Wei Zhou: 0000-0002-5461-3617
Banglin Chen: 0000-0001-8707-8115

Author Contributions

#H.-M.W. and G.C. contributed to this work equally.

Notes

The authors declare no competing financial interest.

■ ACKNOWLEDGMENTS

This work was supported by Grant AX-1730 from the Welch Foundation (BC).

■ REFERENCES

(1) Furukawa, H.; Cordova, K. E.; O'Keeffe, M.; Yaghi, O. M. *Science* **2013**, *341*, 974−987.
(2) Sumida, K.; Rogow, D. L.; Mason, J. A.; McDonald, T. M.; Bloch, E. D.; Herm, Z. R.; Bae, T.-H.; Long, J. R. *Chem. Rev.* **2012**, *112*, 724−781.
(3) Li, J.-R.; Sculley, J.; Zhou, H.-C. *Chem. Rev.* **2012**, *112*, 869−932.
(4) He, Y.; Zhou, W.; Qian, G.; Chen, B. *Chem. Soc. Rev.* **2014**, *43*, 5657−5678.
(5) Li, B.; Wen, H.-M.; Cui, Y.; Zhou, W.; Qian, G.; Chen, B. *Adv. Mater.* **2016**, *28*, 8819−8860.
(6) Férey, G.; Serre, C. *Chem. Soc. Rev.* **2009**, *38*, 1380−1399.
(7) Zhang, J.-P.; Liao, P.-Q.; Zhou, H.-L.; Lin, R.-B.; Chen, X.-M. *Chem. Soc. Rev.* **2014**, *43*, 5789−5814.
(8) Cui, Y.; Li, B.; He, H.; Zhou, W.; Chen, B.; Qian, G. *Acc. Chem. Res.* **2016**, *49*, 483−493.
(9) Farha, O. K.; Eryazici, I.; Jeong, N. C.; Hauser, B. G.; Wilmer, C. E.; Sarjeant, A. A.; Snurr, R. Q.; Nguyen, S. T.; Yazaydın, A. Ö.; Hupp, J. T. *J. Am. Chem. Soc.* **2012**, *134*, 15016−15021.
(10) Yuan, D.; Zhao, D.; Sun, D.; Zhou, H.-C. *Angew. Chem., Int. Ed.* **2010**, *49*, 5357−5361.
(11) Cui, X.; Chen, K.; Xing, H.; Yang, Q.; Krishna, R.; Bao, Z.; Wu, H.; Zhou, W.; Dong, X.; Han, Y.; Li, B.; Ren, Q.; Zaworotko, M. J.; Chen, B. *Science* **2016**, *353*, 141−144.
(12) Schneemann, A.; Bon, V.; Schwedler, I.; Senkovska, I.; Kaskel, S.; Fischer, R. A. *Chem. Soc. Rev.* **2014**, *43*, 6062−6096.
(13) Vaidhyanathan, R.; Iremonger, S. S.; Shimizu, G. K. H.; Boyd, P. G.; Alavi, S.; Woo, T. K. *Science* **2010**, *330*, 650−653.
(14) Wang, C.; Liu, D.; Lin, W. *J. Am. Chem. Soc.* **2013**, *135*, 13222−13234.
(15) Li, B.; Chrzanowski, M.; Zhang, Y.; Ma, S. *Coord. Chem. Rev.* **2016**, *307*, 106−129.
(16) Zhang, Z.; Yao, Z.-Z.; Xiang, S.; Chen, B. *Energy Environ. Sci.* **2014**, *7*, 2868−2899.
(17) Fracaroli, A. M.; Furukawa, H.; Suzuki, M.; Dodd, M.; Okajima, S.; Gándara, F.; Reimer, J. A.; Yaghi, O. M. *J. Am. Chem. Soc.* **2014**, *136*, 8863−8866.
(18) An, J.; Geib, S. J.; Rosi, N. L. *J. Am. Chem. Soc.* **2010**, *132*, 38−39.
(19) Zheng, B.; Bai, J.; Duan, J.; Wojtas, L.; Zaworotko, M. J. *J. Am. Chem. Soc.* **2011**, *133*, 748−751.
(20) Luo, F.; Yan, C.; Dang, L.; Krishna, R.; Zhou, W.; Wu, H.; Dong, X.; Han, Y.; Hu, T.-L.; O'Keeffe, M.; Wang, L.; Luo, M.; Lin, R.-B.; Chen, B. *J. Am. Chem. Soc.* **2016**, *138*, 5678−5684.
(21) Zhang, H.-X.; Liu, M.; Wen, T.; Zhang, J. *Coord. Chem. Rev.* **2016**, *307*, 255−266.
(22) Zhang, J.-P.; Zhu, A.-X.; Lin, R.-B.; Qi, X.-L.; Chen, X.-M. *Adv. Mater.* **2011**, *23*, 1268−1271.
(23) Li, B.; Wen, H.-M.; Zhou, W.; Xu, J. Q.; Chen, B. *Chem.* **2016**, *1*, 557−580.
(24) Bao, S.-J.; Krishna, R.; He, Y.-B.; Qin, J.-S.; Su, Z.-M.; Li, S.-L.; Xie, W.; Du, D.-Y.; He, W.-W.; Zhang, S.-R.; Lan, Y.-Q. *J. Mater. Chem. A* **2015**, *3*, 7361−7367.
(25) Du, L.; Lu, Z.; Zheng, K.; Wang, J.; Zheng, X.; Pan, Y.; You, X.; Bai, J. *J. Am. Chem. Soc.* **2013**, *135*, 562−565.
(26) Xiong, Y.; Fan, Y.-Z.; Yang, R.; Chen, S.; Pan, M.; Jiang, J.-J.; Su, C.-Y. *Chem. Commun.* **2014**, *50*, 14631−14634.
(27) Jia, J.; Wang, L.; Zhu, G. *Chem.—Eur. J.* **2014**, *20*, 9073−9080.
(28) Yoon, J. W.; Chang, H.; Lee, S.-J.; Hwang, Y. K.; Hong, D.-Y.; Lee, S.-K.; Lee, J. S.; Jang, S.; Yoon, T.-U.; Kwac, K.; Jung, Y.; Pillai, R. S.; Faucher, F.; Vimont, A.; Daturi, M.; Ferey, G.; Serre, C.; Maurin, G.; Bae, Y.-S.; Chang, J.-S. *Nat. Mater.* **2016**, DOI: 10.1038/nmat4825.
(29) Bloch, E. D.; Queen, W. L.; Krishna, R.; Zadrozny, J. M.; Brown, C. M.; Long, J. R. *Science* **2012**, *335*, 1606−1610.
(30) Sato, H.; Kosaka, W.; Matsuda, R.; Hori, A.; Hijikata, Y.; Belosludov, R. V.; Sakaki, S.; Takata, M.; Kitagawa, S. *Science* **2014**, *343*, 167−170.
(31) Yang, S.; Ramirez-Cuesta, A. J.; Newby, R.; Garcia-Sakai, V.; Manuel, P.; Callear, S. K.; Campbell, S. I.; Tang, C. C.; Schröder, M. *Nat. Chem.* **2015**, *7*, 121−129.
(32) Li, B.; Wen, H.-M.; Zhou, W.; Chen, B. *J. Phys. Chem. Lett.* **2014**, *5*, 3468−3479.
(33) Chen, K.-J.; Madden, D. G.; Pham, T.; Forrest, K. A.; Kumar, A.; Yang, Q.-Y.; Xue, W.; Space, B.; Perry, J. J.; Zhang, J.-P.; Chen, X.-M.; Zaworotko, M. J. *Angew. Chem., Int. Ed.* **2016**, *55*, 10268−10272.
(34) Jiang, H.-L.; Makal, T. A.; Zhou, H.-C. *Coord. Chem. Rev.* **2013**, *257*, 2232−2249.
(35) Nugent, P.; Belmabkhout, Y.; Burd, S. D.; Cairns, A. J.; Luebke, R.; Forrest, K.; Pham, T.; Ma, S.; Space, B.; Wojtas, L.; Eddaoudi, M.; Zaworotko, M. J. *Nature* **2013**, *495*, 80−84.
(36) Assen, A. H.; Belmabkhout, Y.; Adil, K.; Bhatt, P. M.; Xue, D.-X.; Jiang, H.; Eddaoudi, M. *Angew. Chem., Int. Ed.* **2015**, *54*, 14353−14358.
(37) He, Y.; Li, B.; O'Keeffe, M.; Chen, B. *Chem. Soc. Rev.* **2014**, *43*, 5618−5656.
(38) Xiang, S.; He, Y.; Zhang, Z.; Wu, H.; Zhou, W.; Krishna, R.; Chen, B. *Nat. Commun.* **2012**, *3*, 954−963.
(39) Shekhah, O.; Belmabkhout, Y.; Chen, Z.; Guillerm, V.; Cairns, A.; Adil, K.; Eddaoudi, M. *Nat. Commun.* **2014**, *5*, 4228.
(40) Cadiau, A.; Adil, K.; Bhatt, P. M.; Belmabkhout, Y.; Eddaoudi, M. *Science* **2016**, *353*, 137−140.
(41) Hu, T.-L.; Wang, H.; Li, B.; Krishna, R.; Wu, H.; Zhou, W.; Zhao, Y.; Han, Y.; Wang, X.; Zhu, W.; Yao, Z.; Xiang, S.; Chen, B. *Nat. Commun.* **2015**, *6*, 7328.
(42) Zhao, X.; Bu, X.; Zhai, Q.-G.; Tran, H.; Feng, P. *J. Am. Chem. Soc.* **2015**, *137*, 1396−1399.
(43) Zhao, X.; Bu, X.; Nguyen, E. T.; Zhai, Q.-G.; Mao, C.; Feng, P. *J. Am. Chem. Soc.* **2016**, *138*, 15102−15105.

DOI: 10.1021/acs.cgd.7b00111
Cryst. Growth Des. 2017, 17, 2172−2177

(44) Ding, N.; Li, H.; Feng, X.; Wang, Q.; Wang, S.; Ma, L.; Zhou, J.; Wang, B. *J. Am. Chem. Soc.* **2016**, *138*, 10100−10103.
(45) Gamage, N.-D. H.; McDonald, K. A.; Matzger, A. J. *Angew. Chem., Int. Ed.* **2016**, *55*, 12099−12103.
(46) Zhang, Z. J.; Nguyen, H. T. H.; Miller, S. A.; Ploskonka, A. M.; DeCoste, J. B.; Cohen, S. M. *J. Am. Chem. Soc.* **2016**, *138*, 920−925.
(47) Chen, D.-M.; Tian, J.-Y.; Liu, C.-S.; Du, M. *Chem. Commun.* **2016**, *52*, 8413−8416.
(48) Das, M. C.; Guo, Q.; He, Y.; Kim, J.; Zhao, C.-G.; Hong, K.; Xiang, S.; Zhang, Z.; Thomas, K. M.; Krishna, R.; Chen, B. *J. Am. Chem. Soc.* **2012**, *134*, 8703−8710.
(49) Wang, C.; Li, L.; Tang, S.; Zhao, X. *ACS Appl. Mater. Interfaces* **2014**, *6*, 16932−16940.
(50) Burtch, N. C.; Jasuja, H.; Dubbeldam, D.; Walton, K. S. *J. Am. Chem. Soc.* **2013**, *135*, 7172−7180.
(51) Li, L.; Bell, J. G.; Tang, S.; Lv, X.; Wang, C.; Xing, Y.; Zhao, X.; Thomas, K. M. *Chem. Mater.* **2014**, *26*, 4679−4695.
(52) Hu, Z.; Nalaparaju, A.; Peng, Y.; Jiang, J.; Zhao, D. *Inorg. Chem.* **2016**, *55*, 1134−1141.
(53) Hu, Z.; Zhang, K.; Zhang, M.; Guo, Z.; Jiang, J.; Zhao, D. *ChemSusChem* **2014**, *7*, 2791−2795.
(54) Makal, T. A.; Wang, X.; Zhou, H.-C. *Cryst. Growth Des.* **2013**, *13*, 4760−4768.
(55) Xia, T.; Wang, H.; Duan, X.; Cui, Y.; Yang, Y.; Qian, G. *Microporous Mesoporous Mater.* **2015**, *215*, 109−115.
(56) Bhattacharya, S.; Gubbins, K. E. *Langmuir* **2006**, *22*, 7726−7731.
(57) Xiang, S.; Zhou, W.; Gallegos, J. M.; Liu, Y.; Chen, B. *J. Am. Chem. Soc.* **2009**, *131*, 12415−12419.
(58) Xiang, S.; Zhou, W.; Zhang, Z.; Green, M. A.; Liu, Y.; Chen, B. *Angew. Chem., Int. Ed.* **2010**, *49*, 4615−4618.
(59) Spanopoulos, I.; Bratsos, I.; Tampaxis, C.; Vourloumis, D.; Klontzas, E.; Froudakis, G. E.; Charalambopoulou, G.; Steriotis, T. A.; Trikalitis, P. N. *Chem. Commun.* **2016**, *52*, 10559−10562.
(60) Song, C.; Hu, J.; Ling, Y.; Feng, Y.; Krishna, R.; Chen, D.-l.; He, Y. *J. Mater. Chem. A* **2015**, *3*, 19417−19426.
(61) Song, C.; He, Y.; Li, B.; Ling, Y.; Wang, H.; Feng, Y.; Krishna, R.; Chen, B. *Chem. Commun.* **2014**, *50*, 12105−12108.
(62) Zhang, M.; Wang, Q.; Lu, Z.; Liu, H.; Liu, W.; Bai, J. *CrystEngComm* **2014**, *16*, 6287−6290.
(63) Cai, J.; Wang, H.; Wang, H.; Duan, X.; Wang, Z.; Cui, Y.; Yang, Y.; Chen, B.; Qian, G. *RSC Adv.* **2015**, *5*, 77417−77422.
(64) Zheng, B.; Liu, H.; Wang, Z.; Yu, X.; Yi, P.; Bai, J. *CrystEngComm* **2013**, *15*, 3517−3520.
(65) Alsmail, N. H.; Suyetin, M.; Yan, Y.; Cabot, R.; Krap, C. P.; Lu, J.; Easun, T. L.; Bichoutskaia, E.; Lewis, W.; Blake, A. J.; Schröder, M. *Chem. - Eur. J.* **2014**, *20*, 7317−7324.
(66) Prasad, T. H.; Hong, D. H.; Suh, M. P. S. *Chem. - Eur. J.* **2010**, *16*, 14043−14050.
(67) Kennedy, R. D.; Krungleviciute, V.; Clingerman, D. J.; Mondloch, J. E.; Peng, Y.; Wilmer, C. E.; Sarjeant, A. A.; Snurr, R. Q.; Hupp, J. T.; Yildirim, T.; Farha, O. K.; Mirkin, C. A. *Chem. Mater.* **2013**, *25*, 3539−3543.
(68) Caskey, S. R.; Wong-Foy, A. G.; Matzger, A. J. *J. Am. Chem. Soc.* **2008**, *130*, 10870−10871.
(69) Liao, P.-Q.; Chen, H.; Zhou, D.-D.; Liu, S.-Y.; He, C.-T.; Rui, Z.; Ji, H.; Zhang, J.-P.; Chen, X.-M. *Energy Environ. Sci.* **2015**, *8*, 1011−1016.
(70) Zhai, Q.-G.; Bu, X.; Mao, C.; Zhao, X.; Daemen, L.; Cheng, Y.; Ramirez-Cuesta, A. J.; Feng, P. *Nat. Commun.* **2016**, *7*, 13645.
(71) Li, Y.; Yao, K.; Zhu, Y.; Deng, Z.; Yang, F.; Zhou, X.; Li, G.; Wu, H.; Nijem, N.; Chabal, Y. J.; Lai, Z.; Han, Y.; Shi, Z.; Feng, S.; Li, J. *Angew. Chem., Int. Ed.* **2012**, *51*, 1412−1415.
(72) Lassig, D.; Lincke, J.; Moellmer, J.; Reichenbach, C.; Moeller, A.; Glaser, R.; Kalies, G.; Cychosz, K. A.; Thommes, M.; Staudt, R.; Krautscheid, H. *Angew. Chem., Int. Ed.* **2011**, *50*, 10344−10348.
(73) Li, J.-R.; Yu, J.; Lu, W.; Sun, L.-B.; Sculley, J.; Balbuena, P. B.; Zhou, H.-C. *Nat. Commun.* **2013**, *4*, 1538.
(74) Bao, Z.; Chang, G.; Xing, H.; Krishna, R.; Ren, Q.; Chen, B. *Energy Environ. Sci.* **2016**, *9*, 3612−3641.
(75) Li, L.; Wang, X.; Liang, J.; Huang, Y.; Li, H.; Lin, Z.; Cao, R. *ACS Appl. Mater. Interfaces* **2016**, *8*, 9777−9781.
(76) He, Y.; Zhang, Z.; Xiang, S.; Fronczek, F. R.; Krishna, R.; Chen, B. *Chem. Commun.* **2012**, *48*, 6493−6495.
(77) Zhang, L.; Zou, C.; Zhao, M.; Jiang, K.; Lin, R.; He, Y.; Wu, C.-D.; Cui, Y.; Chen, B.; Qian, G. *Cryst. Growth Des.* **2016**, *16*, 7194−7197.
(78) Demessence, A.; D'Alessandro, D. M.; Foo, M. L.; Long, J. R. *J. Am. Chem. Soc.* **2009**, *131*, 8784−8786.
(79) Zhang, Z.; Li, Z.; Li, J. *Langmuir* **2012**, *28*, 12122−12133.

DOI: 10.1021/acs.cgd.7b00111
Cryst. Growth Des. 2017, 17, 2172−2177